

Thermoelectric power factor enhancement by ionized nanoparticle scattering

Je-Hyeong Bahk,^{1,a)} Zhixi Bian,¹ Mona Zebarjadi,² Parthiban Santhanam,³ Rajeev Ram,³ and Ali Shakouri¹

¹Department of Electrical Engineering, University of California, Santa Cruz, California 95064, USA

²Department of Mechanical Engineering, Massachusetts Institute of Technology, Cambridge, Massachusetts 02139, USA

³Department of Electrical Engineering and Computer Science, Massachusetts Institute of Technology, Cambridge, Massachusetts 02139, USA

(Received 6 May 2011; accepted 27 July 2011; published online 19 August 2011)

We show theoretically that the thermoelectric power factor can be enhanced in degenerate semiconductors when embedded nanoparticles donate carriers to the matrix and replace conventional impurity dopants as scattering centers. Nanoparticle scattering rates calculated by the partial wave method indicate a mobility enhancement over materials with equivalent doping by isolated ionized impurities while the Seebeck coefficient remains nearly intact. We find that the thermoelectric power factor of In_{0.53}Ga_{0.47}As from 300 K to 800 K is enhanced by 15%–30% by nanoparticles 3–4 nm in diameter. © 2011 American Institute of Physics. [doi:10.1063/1.3625950]

The efficiency of thermoelectric energy conversion is directly related to the thermoelectric figure of merit, $ZT = S^2\sigma T / (\kappa_e + \kappa_l)$, of the materials used, where S is the Seebeck coefficient, σ is the electrical conductivity, T is the absolute temperature, and κ_e and κ_l are the electronic and lattice thermal conductivities, respectively. Previously it has been demonstrated that embedded nanoparticles in semiconductors can effectively reduce the lattice thermal conductivity beyond the alloy limit via mid/long wavelength phonon scattering to enhance ZT .¹ However, the numerator in ZT , $S^2\sigma$, the so-called thermoelectric power factor, has not been reported to be noticeably enhanced by such nanoparticles.

There have been several attempts to experimentally and theoretically study the effect of nanoparticles on the thermoelectric power factor.^{2–5} Previous reports have shown that the modified energy-dependent scattering time by electron-nanoparticle interaction can enhance the Seebeck coefficient. However, in these calculations the power factor was at most a few percent enhanced because the electrical conductivity was simultaneously decreased by the addition of scattering by nanoparticles. Recently, Zebarjadi *et al.* studied the effects of size distribution and optimal doping of nanoparticles on the power factor and showed that large enhancement of power factor is possible with 5% volume fraction of metallic nanoparticles in GaAs at low temperatures.⁶ They used the coherent potential approximation method to account for the coherent multiple scattering by nanoparticles at such high nanoparticle volume fractions. In this letter, we focus on the power factor enhancement in materials with nanoparticle low volume fractions at high temperatures.

Efforts to enhance the power factor have mainly focused on enhancing the Seebeck coefficient because enhancements to electrical conductivity are always accompanied by increases in electronic thermal conductivity.^{7,8} Still, in many semiconductors, the lattice thermal conductivity dominates over the electronic contribution. In such cases, increases in the electrical conductivity are accompanied by small frac-

tional increases in total (lattice plus electronic) thermal conductivity and result in ZT enhancement.

Recently, a modulation doping concept has been introduced and experimentally demonstrated in three-dimensional nanostructured bulk materials.⁹ In their work, the sizes of nanograins were much larger than the carrier mean free path, so that the interface scatterings did not alter the scattering time of carriers much. However, when nanograin sizes are comparable to or less than the carrier mean free path, carrier transport can be significantly changed by the nanograin/nanoparticle interface scattering, which therefore must be accurately calculated to study their effects on thermoelectric properties.

It has been recently reported that in Er-doped InGaAs, the carrier density depends strongly on the amount of Er incorporated and that above the solubility limit, where semi-metallic ErAs nano-islands or nanoparticles are formed, Er can dope the matrix to the degenerate regime.^{10,11} Thus, the free carriers in the nanoparticle material result from the ionization of semi-metallic nanoparticles instead of impurity dopants. The size of ErAs nanoparticles is found to be 1–3 nm in diameter, which is much smaller than the electron mean free path (30–70 nm) in InGaAs. As a result, the electrostatic potential around the ErAs nanoparticles must include a screened Coulomb potential to accurately model the scattering of electrons.

The potential profile outside a spherical nanoparticle of radius a , donating Q charges to the matrix, is determined by solving the Poisson equation taking into account the screening effect as

$$V(r) = -\frac{Q}{4\pi\epsilon_s\epsilon_0} \frac{L_D e^{a/L_D}}{a + L_D} \cdot \frac{1}{r} e^{-r/L_D} \quad (r > a), \quad (1)$$

$$= V_0 - \frac{Q}{4\pi\epsilon_s\epsilon_0} \frac{L_D}{a(a + L_D)} = \text{const.} \quad (r < a),$$

where r is the radial distance from the center of nanoparticle, ϵ_s is the static dielectric constant of the matrix, and L_D is the screening length. The factor $L_D e^{a/L_D} / (a + L_D)$ comes from charge neutrality but is close to unity since L_D is normally much larger than a in the doping range of interest. Q is an integer multiple of electron charge, e . Inside the nanoparticle, the potential is taken to be constant as we assume all net

^{a)} Author to whom correspondence should be addressed. Electronic mail: jhbahk@soe.ucsc.edu.

charge lies on the boundary $r = a$ because of the metallic nature of ErAs. There is a potential offset V_0 at the boundary due to the hetero-interface. The inset in Fig. 1 shows the nanoparticle potentials of 1 nm radius with $Q = 1e$ and $2e$ in comparison with the ionized impurity potential. The potential around an ionized impurity diverges to $-\infty$ near the charge center because an ionized impurity is a point charge, whereas the potential for a nanoparticle is truncated at the boundary and becomes constant inside the semi-metallic region. The screened potential tails around nanoparticles are much shorter than the distance between nanoparticles for the low nanoparticle densities of interest. This indicates that electron transport can be assumed only through a single 3D channel in the host matrix instead of percolation.

Fig. 1 shows the electron-nanoparticle scattering (NPS) times for various particle sizes and Q factors. The calculations are based on the partial wave method, which can accurately solve the scattering problem for arbitrary spherically symmetric potential profiles. Details about the partial wave method are described elsewhere.⁴ The partial wave method works well for dilute systems where the distance between nanoparticles is sufficiently large so that each scattering can be treated independently. In Fig. 1, the same carrier density (N_e) of $1 \times 10^{18} \text{ cm}^{-3}$ is used for every curve. For a given Q , the required density of nanoparticles (N_{np}) is obtained from the definition of Q as $Q = e(N_e/N_{np})$. When Q is larger than $1e$, indicating that a nanoparticle donates more than one electron, the nanoparticle scattering becomes stronger than the ionized impurity scattering at the same doping density due to the stronger Coulomb potential, so no enhancement in mobility and power factor is observed. However, for $Q = 1e$, the nanoparticle scattering is weaker than the ionized impurity scattering as shown in Fig. 1. This is because the nanoparticle potential does not possess the very deep well near the scattering center that strongly attracts electrons to ionized impurities. When the nanoparticle radius is smaller than 0.5 nm, its scattering is almost identical to the ionized impurity scattering. For larger nanoparticles, the scattering time increases with increasing radius over most of the energy range of interest. However, for radii 2.0 nm and larger, the scattering time starts to roll over at high energies.

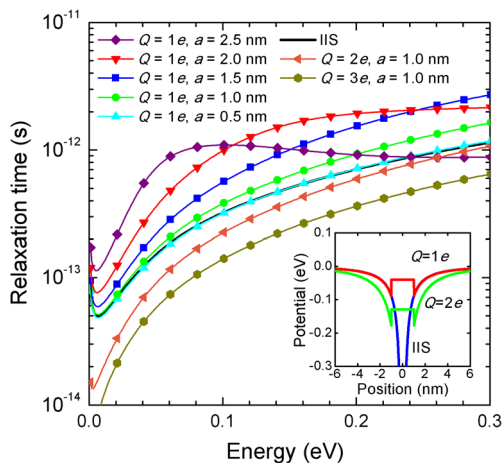


FIG. 1. (Color online) Nanoparticle scattering times for various charge states Q and nanoparticle radii a . Ionized impurity scattering time (IIS) shown for comparison is almost completely overlapped with the curve of $Q = 1e$, $a = 0.5$ nm. (Inset: the nanoparticle potentials for $Q = 1e$ and $2e$ as examples and the ionized impurity (IIS) potential.)

In analogy with the Rayleigh scattering of light, the scattering is stronger for shorter-wavelength electrons with greater momentum and energy.¹² However, this effect is negligible for electrons in the energy range of interest when the nanoparticle size is too small compared to the electron wavelength.

A simple explanation for the observed dependence of scattering time on nanoparticle size presents itself. Examination of nanoparticle scattering under the Born Approximation leads to the conclusion that low-frequency Fourier components of a scattering site's potential profile are responsible for the scattering between states with small differences in their momentum. As a result, the slowly varying screened Coulomb potential tail in our nanoparticle model is responsible for the sharp dip in the scattering time at low energies as compared with the long scattering times for high energy electrons, just as in ionized impurity scattering. On the other hand, the sharp discontinuity at the hetero-interface in the nanoparticle potential from Eq. (1) is responsible for most of the high-frequency Fourier components and should therefore be responsible for most scattering of high-energy electrons. In the Rayleigh regime, we may expect that at high energy the scattering rate should scale as a^6 based on the Born approximation,¹² which is clearly shown in Fig. 1 for scattering by large nanoparticles at high energy.

To achieve a large thermoelectric power factor, a long scattering time is preferred for high electrical conductivity, and a large scattering parameter r , defined by the energy-dependence of the scattering time as $\tau(E) = \tau_0 E^r$, results in a large Seebeck coefficient. At a given energy, the slope of each curve in Fig. 1 is directly proportional to the scattering parameter. As the nanoparticle radius increases from 0.5 nm to 1.5 nm, both the scattering time and the scattering parameter increase, and therefore the power factor can be enhanced. However, if the radius further increases beyond 1.5 nm, the scattering time starts to decrease with energy at high energies due to the Rayleigh scattering. For these larger nanoparticles, the scattering parameter also decreases and eventually becomes negative, resulting in a diminished power factor. We therefore conclude that an optimal nanoparticle size exists to maximize the thermoelectric power factor.

Fig. 2 shows the electrical conductivity, Seebeck coefficient, and power factor of $\text{In}_{0.53}\text{Ga}_{0.47}\text{As}$ as a function of carrier density at 300 K for various nanoparticle sizes, calculated based on the Boltzmann transport equation under the relaxation time approximation.¹³ It has recently been reported that rare-earth doped InGaAlAs has achieved a $ZT \sim 1.3$ at 800 K.⁵ In the III-V semiconductor, the ionized impurity scattering can be a dominant scattering in the material so that the replacing nanoparticle scattering can make a big impact in mobility. However, for materials such as PbTe in which phonon scattering is dominant, the nanoparticle scattering effect may not be very large. Other major scattering mechanisms such as polar optical phonon scattering, acoustic phonon scattering, and alloy scattering are included in the total scattering calculation as described in Ref. 13. A non-parabolic band model is used for the host material.

Over most of the range of interest, the electrical conductivity is enhanced with nanoparticle scattering compared to the case of ionized impurity scattering. At large degenerate carrier concentrations, the diminished electrical conductivity in materials with large nanoparticles of $a = 2.0$ and 2.5 nm is

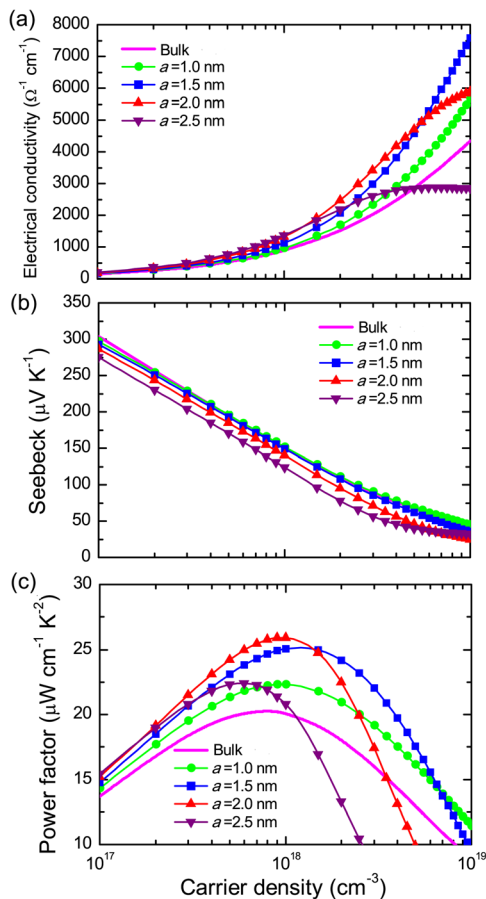


FIG. 2. (Color online) (a) Electrical conductivity, (b) Seebeck coefficient, and (c) thermoelectric power factor of $\text{In}_{0.53}\text{Ga}_{0.47}\text{As}$ with NPS of different sizes in comparison with bulk at 300 K.

expected from the scattering time curves in Fig. 1, since Rayleigh-like scattering figures prominently for the high-energy electrons near the Fermi surface which dominate conduction. Meanwhile, the Seebeck coefficient is only slightly reduced or even slightly increased for the nanoparticles of 0.5 nm–1.5 nm. This is due to the increase in scattering parameter from nanoparticle scattering. Finally, the maximum power factor is calculated to be $26 \mu\text{W}/\text{cmK}^2$ for the particle size of 2.0 nm at the carrier density of $1 \times 10^{18} \text{cm}^{-3}$. This is a 30% enhancement compared to the maximum power factor, $20 \mu\text{W}/\text{cmK}^2$, obtained without nanoparticles at 300 K.

The electronic thermal conductivity is also increased at the same rate as the electrical conductivity. With the optimal particle size at the optimal carrier density, the electronic thermal conductivity is calculated to increase from 0.6 to 0.8 W/mK at 300 K, while the lattice thermal conductivity is taken to be fixed at 5 W/mK. Thus, the total thermal conductivity rises from 5.6 to 5.8 W/mK, corresponding to an increase of just 4%. Since this change is much smaller than the power factor enhancement of 30%, the overall ZT enhancement remains 25%. Note that this ZT enhancement does not include the lattice thermal conductivity reduction by the nanoparticles reported in Ref. 1. Therefore, the overall ZT enhancement could be much larger in nanoparticle materials.

The power factor can be enhanced at higher temperatures as well. Fig. 3 shows the optimal power factors for materials with embedded nanoparticles whose radii are 1.5 and 2.0 nm as a function of temperature from 300 K to 800 K in compari-

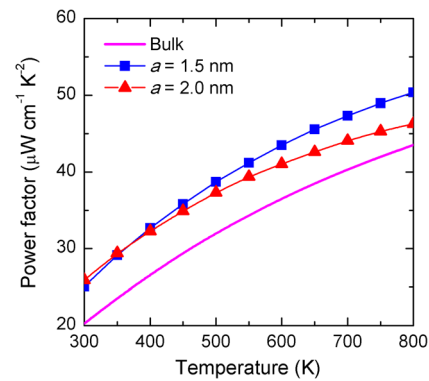


FIG. 3. (Color online) Optimal power factors for $\text{In}_{0.53}\text{Ga}_{0.47}\text{As}$ incorporating nanoparticles with radii of 1.5 and 2.0 nm as a function of temperature in comparison with the optimal values for bulk.

son with the best bulk values. The optimum power factor for the material with nanoparticles with a radius of 2.0 nm becomes smaller than that of 1.5 nm radius at high temperatures, because the Rayleigh scattering has a more substantial contribution at high temperatures for larger nanoparticles. The percentage of enhancement in power factor gradually decreases from 30% to 15% with temperature increasing from 300 K to 800 K due to the increased phonon scattering rate at high temperature, which reduces the relative importance of nanoparticle scattering in the total scattering time.

In summary, the optimized nanoparticle scattering in replacement of ionized impurity scattering can enhance the thermoelectric power factor by 15%–30% in the semiconductor alloy $\text{In}_{0.53}\text{Ga}_{0.47}\text{As}$ over the temperature range of 300 K to 800 K. This is the combined effect of the enhanced mobility by the increased relaxation time and the strong energy dependence of nanoparticle scattering that helps to maintain the high Seebeck coefficient. There is an optimal size of nanoparticles, which is found to be 3–4 nm in diameter, above which both the electrical conductivity and Seebeck coefficient can be decreased due to the Rayleigh scattering of electrons off large particles.

This work was partly supported by DARPA/NMP.

- ¹W. Kim, J. Zide, A. Gossard, D. Klenov, S. Stemmer, A. Shakouri, and A. Majumdar, *Phys. Rev. Lett.* **96**, 045901 (2006).
- ²J. P. Heremans, C. M. Thrush, and D. T. Morelli, *Phys. Rev. B* **70**, 115334 (2004).
- ³S. V. Faleev, and F. Leonard, *Phys. Rev. B* **77**, 214304 (2008).
- ⁴M. Zebarjadi, K. Esfarjani, A. Shakouri, J.-H. Bahk, Z. Bian, G. Zeng, J. E. Bowers, H. Lu, J. M. O. Zide, and A. C. Gossard, *Appl. Phys. Lett.* **94**, 202105 (2009).
- ⁵J. M. O. Zide, J.-H. Bahk, R. Singh, M. Zebarjadi, G. Zeng, H. Lu, J. P. Feser, D. Xu, S. L. Singer, Z. X. Bian, A. Majumdar, J. E. Bowers, A. Shakouri, and A. C. Gossard, *J. Appl. Phys.* **108**, 123702 (2010).
- ⁶M. Zebarjadi, K. Esfarjani, Z. Bian, and A. Shakouri, *Nano Lett.* **11**, 225 (2011).
- ⁷L. D. Hicks and M. S. Dresselhaus, *Phys. Rev. B* **47**, 1272 (1993).
- ⁸J. P. Heremans, V. Jovovic, E. S. Toberer, A. Saramat, K. Kurosaki, K. Charoenphakdee, S. Yamanaka, and J. F. Snyder, *Science* **321**, 554 (2008).
- ⁹M. Zebarjadi, G. Joshi, G. Zhu, B. Yu, A. Minnich, Y. Lan, X. Wang, M. Dresselhaus, Z. Ren, and G. Chen, *Nano Lett.* **11**, 2225 (2011).
- ¹⁰D. C. Driscoll, M. Hanson, C. Kadow, and A. C. Gossard, *Appl. Phys. Lett.* **78**, 1703 (2001).
- ¹¹P. Burke, H. Lu, N. G. Rudawski, A. C. Gossard, J.-H. Bahk, and J. E. Bowers, *J. Vac. Sci. Technol. B* **29**(3), 03C117(2011).
- ¹²H. C. van de Hulst, *Light Scattering by Small Particles* (John Wiley, New York, 1957).
- ¹³J.-H. Bahk, Z. Bian, M. Zebarjadi, J. M. O. Zide, H. Lu, D. Xu, J. P. Feser, G. Zeng, A. Majumdar, A. C. Gossard, A. Shakouri, and J. E. Bowers, *Phys. Rev. B* **81**, 235209 (2010).